IJE TRANSACTIONS A: Basics Vol. 39, No. 10, (October 2026) 2485-2499

International Journal of Engineering

Journal Homepage: www.ije.ir

A Deep Learning Based Signal Detection Framework for Non Orthogonal Multiple Access Systems

M. Tulasi[a,b], D. Sreenivasa Rao*[a]

[a] *Department of Electronics and Communication Engineering, Koneru Lakshmaiah Education Foundation, Vaddeswaram, AP, India*
[b] *Department of DTDP, Dr. YSR Architecture and Fine Arts University, Kadapa, AP, India*

PAPER INFO

Paper history:
Received 01 September 2025
Received in revised form 27 September 2025
Accepted 24 October 2025

Keywords:
Neural Network Architecture
Pilot-Aware Detection Signal Demodulation
Wireless Access Technology
Symbol Error Rate

ABSTRACT

This paper presents GVDET-Net, an innovative signal detection framework designed to enhance the detection accuracy and operational efficiency of NOMA systems utilizing non-orthogonal time-frequency resources. The proposed model integrates VGG19-based CNN layers with GRU layers to jointly extract spatial and temporal dependencies from input data. By sequentially processing hierarchical features, GVDET-Net achieves superior NOMA channel signal detection compared to ML, LS, and MMSE approaches across SNRs from 4 dB to 28 dB. Simulation results demonstrate its effectiveness under realistic NOMA conditions, outperforming SIC-LS and SIC-MMSE under multiple test scenarios with 64 and 16 pilot configurations for dual-user cases. GVDET-Net achieves a minimum Symbol Error Rate (SER) of approximately 10^{-3} at high SNR levels, delivering significant performance gains. Additionally, the model attains 96.4% classification accuracy, 3.1 ms inference latency for standard packet sizes, and an AUC score of 0.968, validating its robustness and real-time applicability. This work introduces advanced detection techniques for NOMA systems, paving the way for optimized wireless networks and supporting next-generation communication standards.

***doi**: 10.5829/ije.2026.39.10a.11*

Graphical Abstract

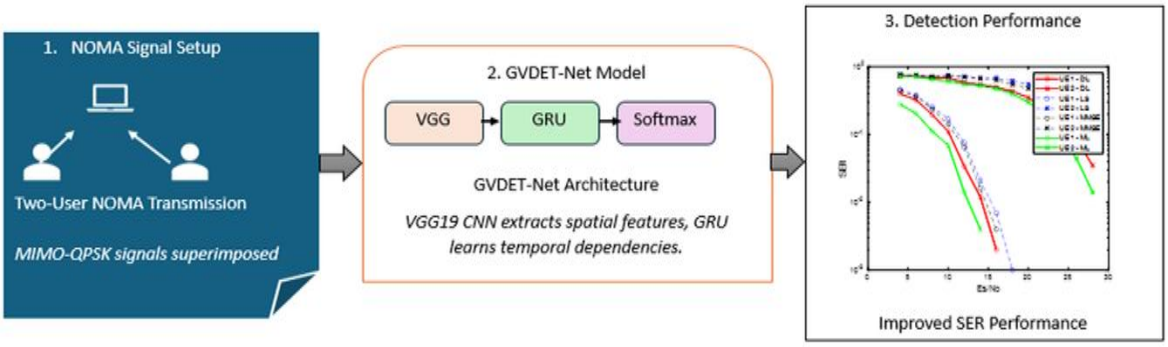

NOMENCLATURE

N_CP	Length of Cyclic Prefix	N_PSC	Number of Pilot Subcarriers
N_UE	Number of Users (User Equipments)	N_SC	Number of Subcarriers
N_PSym	Number of Pilot OFDM Symbols per Packet	N_DSym	Number of Data OFDM Symbols per Packet
d_i	Modulated Data Symbol (QPSK)	a_i, b_i	Amplitude components of QPSK symbols
N_0	Noise Power	σ^2	Noise Variance

*Corresponding Author Email: sreenuece@kluniversity.in (D. Sreenivasa Rao)

Please cite this article as: Tulasi M, Sreenivasa Rao D. A Deep Learning Based Signal Detection Framework for Non Orthogonal Multiple Access Systems. International Journal of Engineering, Transactions A: Basics. 2026;39(10):2485-99.

1. INTRODUCTION

The growing demand, along with increasing system capacity requirements, has led to the development of new wireless communication technologies (1). The wireless industry has recognized the potential of Non-Orthogonal Multiple Access (NOMA) technology, which offers distinct functionalities compared to traditional Orthogonal Frequency Division Multiplexing (OFDM) systems (2-5). This shift in the communication paradigm provides several advantages, such as enhanced spectral efficiency, increased system capacity, and more equitable resource distribution (6-8). NOMA achieves these benefits through power domain multiplexing, allowing multiple users to transmit simultaneously on the same resources, thereby maximizing spectrum utilization (9). Additionally, NOMA dynamically adjusts its resource distribution based on user channel conditions to improve system performance and operational efficiency (10).

The wireless communication sector adopts NOMA because it significantly enhances spectral efficiency while expanding system capacity and implementing fair resource distribution and adaptive resource allocation strategies (11). NOMA makes full use of the available spectrum, enabling users to transmit information concurrently (12). As a result, maximum throughput and increased user capacity can be achieved within the same bandwidth allocation (13-14). The resource allocation mechanism optimizes resource utilization according to individual user conditions, ensuring that users have equitable access to network resources despite varying data demands and changing channel conditions.

The compatibility of NOMA with emerging technologies such as massive MIMO and millimeter-wave (mmWave) communications makes it a highly attractive solution.

Current signal detection technology in NOMA systems relies on Machine Learning (ML) and Deep Learning (DL) methods to analyze large datasets and extract valuable features. However, signal detection in NOMA systems presents inherent challenges due to interference and variable channel conditions, as these systems share resources non-orthogonally among multiple users.

These algorithms leverage historical data analysis to identify incoming signals from various users while minimizing interference through pattern detection in received signals. Proof of concept indicates that the sequential pattern analysis and feature extraction capabilities of deep learning models make them well suited for NOMA signal detection applications. The ability of DL models to enhance detection performance stems from their capacity to recognize complex relationships within extensive datasets that include received signals along with corresponding user labels. The integration of ML and DL techniques for NOMA signal detection facilitates adaptive resource allocation, as signal characteristics serve as the foundation for determining resource distribution, ultimately improving system performance and efficiency. ML and DL technologies yield robust signal detection outcomes for NOMA systems, significantly enhancing both spectrum availability and overall system performance while increasing potential data rates. Today's communication systems favor NOMA for its ability to deliver high data rates, improved performance, and optimized spectrum utilization.

This research introduces GVDET-Net, a novel signal detection model that combines artificial intelligence techniques with traditional analysis methods. GVDET-Net facilitates deep learning processing by integrating GRU layers with VGG19 CNN layers to effectively track spatial and temporal relationships. The model enhances signal detection outcomes for NOMA channels by utilizing hierarchical features and sequential modeling techniques. Extensive simulations and analytical studies demonstrate how GVDET-Net improves signal detection capabilities and aligns with future wireless network standard optimization.

The paper begins with Section 1, which outlines the study's problem, significance, and objectives, along with a structural overview. Section 2 provides an in-depth review of the existing literature and methodologies relevant to the research. In Section 3, the core components and architectural specifics of our innovative model are detailed, offering a comprehensive exploration of the proposed system. Section 4 presents the results of the experimental outcome analysis, including performance metrics and comparative evaluations. The paper concludes with a summary of the key findings discussed in Section 5.

2. RELATED WORKS

Research in this section highlights several detection approaches developed to address interference and performance challenges in NOMA systems. Kumar et al. (15) proposed a deep learning–based method for managing signals under memory and computational constraints. Using gradient descent for parameter optimization, their work emphasized the impact of dataset diversity and computational complexity on detection accuracy, while also noting practical limitations in hardware and algorithmic scalability.

Astharini et al. (16) implemented trellis-coded detection in NOMA, demonstrating reduced interference and improved spectral efficiency. However, their approach was sensitive to environmental conditions and decoding complexity, which limit real-time applicability.

Kandasamy et al. (17) applied Support Vector Machines (SVM) for NOMA signal detection over Rayleigh fading channels. While SVM provided robustness to noise and nonlinear decision boundaries, it struggled with closely spaced users and dynamic fading, leading to reduced accuracy.

Salari et al. (18) introduced clustering-based detection to mitigate interference in NOMA. Despite performance gains, the method required careful tuning of cluster parameters and faced difficulties in highly dynamic channel environments. Lin et al. (19) developed a sparse CNN-based demodulation approach, improving computational efficiency but sacrificing the ability to capture fine-grained signal variations, especially under poor channel conditions. Finally, Chuan Lin et al. (20) explored deep learning for MIMO-NOMA detection using a modified LeNet-5 architecture. While effective in capturing spatial dependencies, the shallow network structure limited its ability to model complex, high-dimensional channel characteristics. Together, these studies highlight the progress and limitations of existing methods, motivating the need for a hybrid deep learning framework like GVDET-Net that can jointly capture spatial and temporal features while remaining computationally efficient.

Successive Interference Cancellation (SIC) combined with classical estimators such as Least Squares (LS) and Minimum Mean Square Error (MMSE) has been extensively employed as a benchmark method in NOMA detection research. For example, McWade et al. (21) studied OTFS-NOMA detection schemes and used MMSE-SIC as a baseline to evaluate symbol error rate performance. Similarly, Rahman et al. (22) proposed a Bi-LSTM-based joint detection model in NOMA-OFDM and compared it against LS-SIC and MMSE-SIC, highlighting their limitations in Rayleigh fading channels. While alternative schemes such as Maximum Likelihood (ML) or message-passing detection exist, they are often computationally prohibitive or scenario-specific, making SIC-based methods the most widely accepted practical benchmarks. Thus, our choice of SIC-LS and SIC-MMSE as comparators ensures consistency with established literature.

Successive Interference Cancellation (SIC) combined with classical estimators such as Least Squares (LS) and Minimum Mean Square Error (MMSE) has been widely utilized as a benchmark method in Non-Orthogonal Multiple Access (NOMA) detection research. For instance, McWade et al. (21) explored OTFS-NOMA detection schemes and employed MMSE-SIC as a baseline to assess the performance of the symbol error rate. Similarly, Rahman et al. (22) introduced a Bi-LSTM-based joint detection model in NOMA-OFDM, comparing it against LS-SIC and MMSE-SIC while highlighting their limitations in Rayleigh fading channels. Although alternative approaches like Maximum Likelihood (ML) or message-passing detection are available, they tend to be computationally intensive or specific to certain scenarios, which positions SIC-based methods as the most widely accepted practical benchmarks. Consequently, our selection of SIC-LS and SIC-MMSE as comparators aligns with established literature.

3. METHODOLOGY

The GVDET-Net architecture introduces a novel signal detection approach for Non-Orthogonal Multiple Access (NOMA) systems. The second crucial section of our proposed system implements VGG19 Convolutional Neural Network (CNN) layers in conjunction with Gated Recurrent Unit (GRU) layers to capture the spatial and temporal relationships embedded in the input data.

Initially, the model utilizes a pre-trained VGG19 for feature extraction to identify patterns at the layer level. This information is then passed to the GRU layers to facilitate sequence processing from a contextual perspective. The integration of these model components enhances signal detection by leveraging space-time information, resulting in improved performance and adaptability for complex communication operations.

The proposed system workflow is illustrated in Figure 1. System parameters are employed to generate training data through QPSK modulation, followed by virtual simulations of the transmission and reception processes. The training of GVDET-Net is conducted using the prepared data, while developers define the specific structure of the network and the criteria for adjustments before initiating the training operations. The final phase includes testing and evaluating the system through a series of assessments that utilize replicated testing data, applying detection methods such as Machine Learning (ML), Least Squares (LS), Minimum Mean Square Error (MMSE), and the proposed Deep Learning (DL) model (GVDET-Net). Performance outcomes are then assessed across various signal-to-noise ratios. This systematic workflow method allows for comprehensive development, training, and testing of NOMA systems with detection algorithms for two users.

Figure 2 illustrates the complete process flow for generating the training data necessary for signal detection. The process commences with defining system parameters and establishing the modulation scheme for data symbols, specifically MIMO-QPSK modulation. It

Figure 1. Proposed methodology Block Diagram

then calculates noise power and variance based on the provided Es/N0, sets target Signal-to-Noise Ratios (SNR) for each user, and determines power allocation factors for each subcarrier. Following this, random channel realizations and their corresponding frequency responses are generated prior to creating training data for each class. This includes generating fixed pilot symbols, substituting pilot subcarriers, producing data symbols, and simulating data transmission and reception. Feature vectors and labels are created for each symbol combination, and all generated training data—including channel realizations and details of pilot subcarriers—is saved in the "trainData.mat" file for further analysis and use in training neural networks aimed at efficient signal detection in NOMA systems.

The following discussion outlines the process of generating training data, including the necessary equations. Key system parameters that need to be defined are the length of the cyclic prefix, the number of pilot subcarriers, the number of users (UE), the total number of subcarriers, the number of pilot OFDM symbols per packet, and the number of data OFDM symbols per packet.

The notations are provided below:

- Length of Cyclic Prefix: *N*_CP
- Number of Pilot Subcarriers: *N*_PSC
- Number of Users: *N*_UE
- Number of Subcarriers: *N*_SC
- Number of Pilot OFDM Symbols per Packet: *N*_PSym
- Number of Data OFDM Symbols per Packet: *N*_DSym

Define the modulation scheme for data symbols using MIMO-Quadrature Phase Shift Keying (MIMO-QPSK) modulation. In this scheme, each data symbol is modulated using QPSK, which encodes two bits of data into a single symbol by altering the phase of the carrier signal. MIMO systems facilitate the independent modulation of each stream from different antennas.

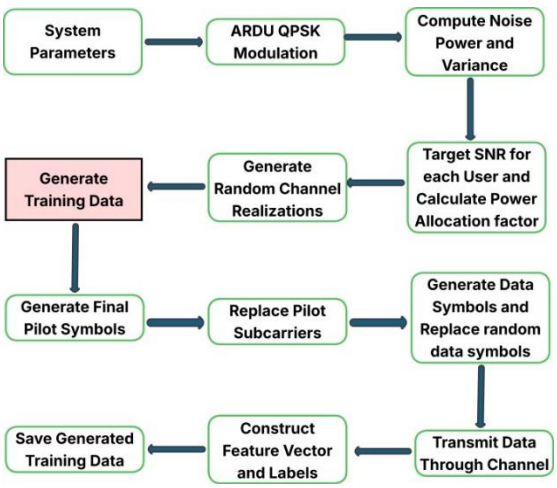

Figure 2. Process flow for creating training data required for signal detection

The complex symbols for QPSK modulation are typically chosen from the set:

$$\{s1 = a + bj, s2 = -a + bj, s3 = -a - bj, s4 = a - b \quad (1)$$

where a and b are the amplitude values, and j represents the imaginary unit.

In the context of MIMO, each data symbol may be independently modulated with one of these complex symbols for transmission over multiple antennas.

Therefore, for MIMO-QPSK modulation, each data symbol *di* is represented as:

$$d_i = a_i + b_i\, j \quad (2)$$

where *i* denotes the specific data symbol, and *ai* and *bi* are the amplitude values for the i^{th} symbol chosen from the set of $\{a,-a\}$ and $\{b,-b\}$, respectively.

These equations describe the modulation scheme for data symbols in MIMO-QPSK modulation within the given system parameters.

The noise power (*N*0) can be computed from the given Es/N0 (signal-to-noise ratio per symbol) in decibels (EsN0_dB) as:

$$N_0 = \frac{E_s}{\mathrm{EsN0_{dB}} \times \mathrm{SymR}} \quad (3)$$

Where *Es* is the symbol energy and SymR is the symbol rate.

Then, the noise variance (σ^2) can be calculated as

$$\sigma^2 = \frac{N_0}{2} \quad (4)$$

Define target Signal-to-Noise Ratio (SNR) for each user and calculate the power allocation factor for each subcarrier. For each user *i*, the target SNR (targetSNR*i*) in decibels can be specified. Let's denote targetSNR*i* as the target SNR for user *i*.

The power allocation factor (powerFactor_*k*,*i*) for each subcarrier *k* and user *i* can be calculated based on the target SNR and channel gain.

$$\mathrm{powerFactor}_{k,i} = \frac{targetSNR_i}{gainH_{k,i}} \quad (5)$$

where $gainH_{k,i}$ is the channel gain for subcarrier *k* and user *i*.

Generate a random channel realization and its corresponding frequency response.

For each user *i* and each subcarrier *k*, a random channel coefficient *h*_*k*,*i* can be generated from a complex Gaussian distribution:

$$hk, i \sim CN(0, \sigma_h^2) \quad (6)$$

σ_h^2 is the variance of the channel coefficients.

The corresponding frequency response *H*_*k*,*i* can be obtained by taking the Discrete Fourier Transform (DFT) of the channel coefficients:

$$H\_k,i = DFT(h_{k,i}) \quad (7)$$

Fixed pilot symbols are created using BPSK modulation for each user to generate training data for signal detection in a two-user NOMA system, and these fixed symbols are then replaced with pilot subcarriers.

For each user i and each packet l, the fixed pilot symbols fixedPilot_i,l can be generated using BPSK modulation:

$$fixedPilot_{i,l} = sign(rand(1, numPSC) - 0.5) \quad (8)$$

Next, data symbols are created, and random data symbols are substituted for the current data combination on the designated target subcarrier. The process then simulates data transmission and reception. Upon reception, feature vectors are created and labels assigned. Finally, all generated training data, including feature vectors, labels, channel realizations, pilot subcarrier details, and so on, is saved in a file called "trainData.mat" for future use and analysis. This comprehensive approach ensures the creation of a strong dataset for training neural networks.

The proposed model architecture presented in Figure 3 is characterized by sequence input, VGG19 layers, a GRU layer with modified parameters, fully connected layers, and softmax and classification layers. These elements together form the neural network framework intended for training purposes. The use of the 'adam' optimizer facilitates the establishment of training options, which necessitate various parameters, including the initial learning rate, execution environment, gradient threshold, learning rate drop factor, mini-batch size, and other related values. The output of the trained deep neural network is saved in the "NN.mat" file, allowing for future evaluations.

Figure 4 illustrates a two-user NOMA system during the testing phase, where performance assessment occurs under varying Signal-to-Noise Ratio (SNR) conditions. The procedure begins with defining the essential system components, which include the number of subcarriers, pilot carrier count, and GVDET-Net model implementation. The system employs MIMO-Quadrature

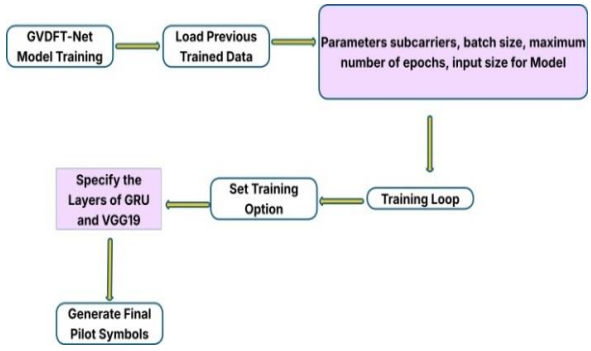

Figure 3. Training Proposed GVDET-Net Model

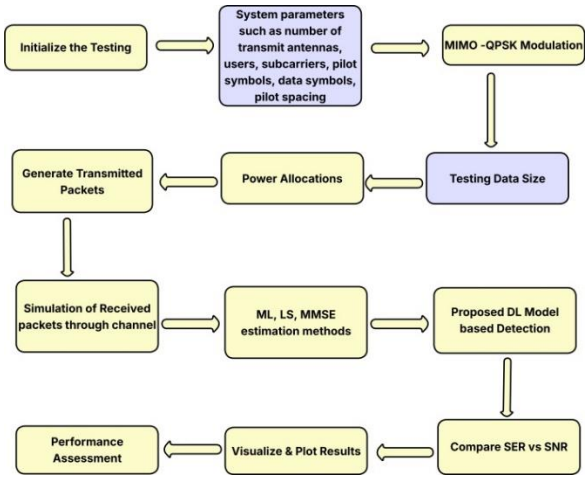

Figure 4. Testing Stage diagram

Phase Shift Keying (QPSK) modulation for data transmission. Subsequently, the testing procedure outlines data sizes and power allocation steps across different SNR conditions to ensure a comprehensive evaluation. Each SNR value is contacted by generating test packets that conform to the training format through fixed pilot patterns and data packet transfers. Packet reception testing enables the assessment of various detection methods by incorporating channel-based simulations and noise processing.

The analysis involves calculating symbol error rates over multiple iterations for each SNR level to ensure accurate performance measurement. The examination of symbol error rates between the proposed detection methods and traditional schemes offers important conclusions about the effectiveness of the detection techniques based on signal-to-noise ratio (SNR) evaluations. The system includes functionality for generating channel covariance matrices by leveraging relevant system parameters, thereby enhancing the realism of the system evaluation. This comprehensive testing approach facilitates in-depth assessments of NOMA system performance by evaluating both detection accuracy and robustness, which ultimately supports practical optimization and refinement processes.

The following paragraphs present a breakdown of the screening procedure together with necessary mathematical components.

Important data must be loaded including training information, the GVDET-Net Model, and its channel covariance matrix. Define system parameters including the number of users, subcarriers, pilot symbols, data symbols, SNR levels, modulation scheme (MIMO-QPSK), as below:

Number of users: N_users
Number of subcarriers: N_subcarriers
Number of pilot symbols: N_pilots
Number of data symbols: N_data_symbols

Signal-to-Noise Ratio: SNR
Modulation Scheme: QPSK
MIMO Configuration: *M*_tx×*M*_rx (antennas)

Generate the channel covariance matrix and compute noise parameters based on the desired SNR levels.

In a MIMO system, the channel matrix \(H \) represents the link between the transmit and receive antennas. Here, a Rayleigh fading channel is considered, in which \(H \)'s elements are complex. The channel covariance matrix \(R_{channel} \) can be calculated as follows:

$$\mathrm{R_{channel}} = \mathrm{E}[\mathrm{HH}^H] \quad (9)$$

where H^H denotes the conjugate transpose of H, and E[·] denotes the expectation operator.

The noise power σnoise2 can be determined from the desired SNR (SNR_db) as follows:

$$\sigma^2_{\mathrm{noise}} = \frac{\sigma^2_{signal}}{SNR} \quad (10)$$

where σ^2_{signal} is the signal power. In an OFDM system, the signal power σ^2_{signal} can be computed as the sum of the powers of the data symbols, assuming unit power per symbol. Generate pilot and data symbols for each user and Combine pilot and data symbols into transmit packets.

Allocate power to users based on the channel gains and target SNR levels. Pilot symbols can be generated using a known sequence, such as a training sequence or a pseudo-random sequence. Let's denote the pilot symbols for user *i* as p*i*, and the data symbols as d*i*. For each user *i*, the transmit packet can be formed by concatenating the pilot symbols p*i* and data symbols d*i*. Let's denote the transmit packet for user *i* as x*i*, then:

$$\boldsymbol{xi} = [\boldsymbol{p}_i \boldsymbol{d}_i] \quad (11)$$

The transmit power for each user can be allocated based on the channel gains and the target SNR levels. Let H*i* denote the channel matrix for user *i*, and SNRtarget*i* denote the target SNR for user *i*. The transmit power *Pi* for user *i* can be computed as:

$$Pi = SNR_{targeti} \times Tr(\boldsymbol{H}_i \boldsymbol{H}_i^H) \quad (12)$$

where Tr(·) denotes the trace of a matrix.

Simulate the transmission and reception process. Add noise to the received signal and estimate the channel using LS and MMSE methods. Next, the process begins with Maximum Likelihood (ML) detection, considering the previously discussed channel knowledge, to decode transmitted symbols. Symbols are then decoded using the Least Squares (LS) and Minimum Mean Square Error (MMSE) estimation techniques. In addition, symbols are decoded using the proposed GVDET-Net Deep Learning (DL) detection, which uses a pre-trained neural network. Following that, the number of symbol errors is determined for each detection method. This entire procedure is repeated at various Signal-to-Noise Ratio (SNR) levels and iterations to assess performance robustness. Finally, the Symbol Error Rates (SER) for each detection method are plotted against the various SNR levels to gain insight into their relative performance under varying noise conditions.

3. 1. Proposed GVDET-Net Model The proposed GVDET-Net architecture offers a novel approach to signal detection in NOMA systems by combining the strengths of VGG19 CNN layers and GRU (Gated Recurrent Unit) layers.

The model effectively captures both spatial and temporal dependencies in the input data by utilizing pre-trained VGG19 layers for feature extraction and pattern recognition, followed by GRU layers for sequential processing and context modeling. This hybrid architecture outperforms traditional methods by integrating VGG19's hierarchical representations with GRU's memory-enhanced capabilities, resulting in more robust and accurate signal detection in NOMA channels.

The GVDET-Net architecture, as shown in Figure 5, begins with an Input Layer, which serves as the entry point for input data. This layer is followed by VGG19 CNN layers, excluding the first (input) and last layers (fully connected and softmax), which are responsible for extracting hierarchical features from the input data. These features capture the intricate patterns and structures present in the received signals. Sequence modeling is then introduced with the addition of GRU layers. The GRU layers, configured with a fixed number of hidden units and an output mode of 'last', enable the network to capture the temporal dependencies and dynamics inherent in signal sequences. This sequential information is critical for understanding the changing nature of signals in NOMA systems. Following the GRU layers, a Fully Connected Layer aggregates features and reduces dimensionality, succeeded by a Softmax Layer to estimate the probability distribution across classes. Finally, a Classification Layer categorizes the extracted features into different signal types or states, facilitating decision-making and evaluation of signal detection performance. Overall, this layered architecture combines deep feature extraction and sequence modeling techniques to enhance signal detection in NOMA systems.

One significant feature of the GVDET-Net is the integration of two powerful neural network architectures for signal detection in NOMA systems. While VGG19 CNN layers excel at extracting complex spatial features from input data, GRU layers can capture temporal dependencies and long-term context information. This combination allows the model to more effectively process the complex dynamics found in NOMA channels, resulting in improved detection performance. Furthermore, the use of pre-trained VGG19 layers

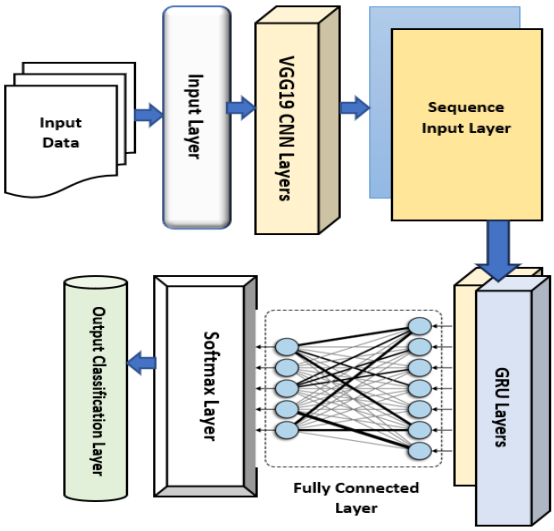

Figure 5. Proposed GVDET-Net Model architecture

enables transfer learning, which reduces the need for large amounts of labeled data and speeds up the training process. Overall, the GVDET-Net represents a novel and promising approach to signal detection in NOMA systems, with the potential to improve the reliability and efficiency of wireless communications networks.

Conventional SIC-based methods, such as LS-SIC and MMSE-SIC, are limited by their reliance on accurate channel estimation and are susceptible to error propagation when initial symbol decisions are incorrect. These limitations cause degraded performance under low SNR or severe fading conditions. Maximum Likelihood (ML) detection achieves optimal SER but is computationally infeasible for large-scale NOMA systems due to its exponential complexity. Similarly, message-passing algorithms and clustering-based detection approaches, while reducing complexity, often introduce additional iterations and overhead, which compromise real-time performance. The proposed GVDET-Net overcomes these limitations by combining VGG19 convolutional layers with GRU temporal modeling to directly learn symbol detection from raw data. This hybrid design reduces sensitivity to imperfect channel estimation, suppresses error propagation through end-to-end learning, and maintains low inference latency. Consequently, GVDET-Net attains robust detection accuracy comparable to optimal methods while remaining computationally efficient for practical NOMA deployments.

The primary distinction between the proposed GVDET-Net and traditional detection methods such as SIC-LS, SIC-MMSE, and Maximum Likelihood (ML) lies in the architecture and robustness to channel conditions. SIC-based approaches depend heavily on accurate channel estimation and suffer from error propagation during successive cancellation, especially under low SNR conditions. In contrast, GVDET-Net employs a hybrid deep learning framework that combines VGG19 convolutional layers for extracting spatial features with GRU layers for modeling temporal dependencies in symbol sequences. This enables the model to capture nonlinear channel effects directly from data, reducing sensitivity to channel estimation errors. Compared to ML detection, which offers optimal SER at the cost of exponential computational complexity, GVDET-Net achieves comparable accuracy while maintaining practical inference latency. Thus, GVDET-Net delivers superior performance across a wide SNR range, combining robustness, efficiency, and scalability for real-world NOMA systems.

3. 2. Algorithm of Proposed AdaptoNet Model

This algorithm, shown below, depicts the *GVDET-Net model* architecture's initialization, training, evaluation, adaption, and interpretation procedures in detail.

4. EXPERIMENTAL INVESTIGATION

The simulation parameters listed in Table 1 are critical components of data testing in signal detection, particularly in Non-Orthogonal Multiple Access (NOMA) systems.

NOMA is a promising multiple access technique that allows multiple users to share the same spectrum resources non-orthogonally, resulting in more efficient spectrum utilization and system capacity. NOMA systems separate users based on power rather than traditional orthogonal time or frequency domains. The specified parameters indicate the simulation setup's complexity and realism. The narrowband Rayleigh fading channel model simulates the real-world wireless

Algorithm: GVDET-Net Model

Algorithm 1. GVDET-Net Signal Detection

1. Input: Received NOMA signal y, channel state H, pilot set P.
2. Preprocessing:
   a. Normalize input signals.
   b. Apply cyclic prefix removal and FFT.
3. Feature Extraction (Spatial):
   a. Pass processed signal through VGG19-based CNN layers.
   b. Extract spatial feature maps.
4. Feature Modeling (Temporal):
   a. Input extracted features into GRU layers.
   b. Capture temporal dependencies across subcarriers.
5. Classification:
   a. Fully connected layer + Softmax for symbol classification.
6. Output: Detected QPSK symbols for User 1 and User 2.

communication environment, in which signals exhibit random amplitude and phase fluctuations due to multipath propagation. Background noise, which is ubiquitous in communication channels, is modeled using additive white Gaussian noise (AWGN).

Advanced modem equipment in NOMA systems utilizes MIMO-QPSK modulation with 64 subcarriers, along with pilot subcarriers to maximize spectral efficiency. In NOMA systems, multiple propagation paths (multipath components) become essential because they account for signal reflections, diffraction, and scattering that occur in wireless channels.

A cyclic prefix of length 16 constitutes an essential determinant for OFDM-based NOMA systems since it decreases the interference between symbols created by multipath propagation. The evaluation of system performance requires 1000 packets while model convergence and learning adequacy become achievable through prolonged training of 50 epochs at specific learning rate and iterations per epoch. The SNR detection scenario operates between 4 dB and 28 dB because these values represent typical working circumstances for NOMA signal detection. NOMA system performance evaluation under signal detection conditions benefits from the combination of these selected experimental parameters.

The training process of the proposed GVDET-Net Model through 50 epochs appears in provided graphs. Figure 6 demonstrates a substantial increase of training accuracy along the time span. The initial accuracy measurement between 5.95% reveals that the model produces erroneous results most of the time. The model achieves major accuracy improvement throughout training so it completes Epoch 4 with perfect 100% accuracy. The training data enables the model to enhance its predictive capabilities until it achieves perfect accuracy rates during Epoch 4.

TABLE 1. Simulation Parameters

Parameter	Value
Channel Model	Narrowband Rayleigh Fading
Noise Model	Additive White Gaussian Noise (AWGN)
Modulation Scheme	MIMO- Quadrature Phase Shift Keying (QPSK)
Subcarriers	64
Pilot Subcarriers	8
No. of Paths	3
Cyclic Prefix Length	16
Testing Dataset Packets	1000
Training Epochs	50
Learning Rate	0.01
Iterations per Epoch	120
SNR Range	4 dB to 28 dB

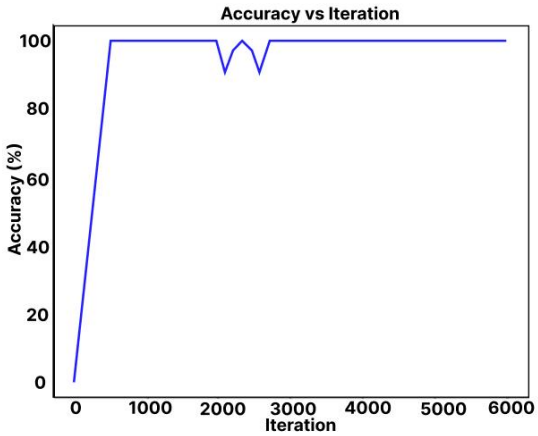

Figure 6. Training Accuracy at 50 Epochs

Training loss performance data shown in Figure 7 enhances the accuracy graph by showing the model reaches its best solution. The model initially produces large amount of loss because its predictions contain substantial mistakes. For every training step the model demonstrates decreased loss until reaching an optimal point for minimizing predictive errors. Training loss descends during all training sessions before reaching a stable value of 0.025. When loss reaches a low point the model demonstrates successful training from training data while any additional modifications will have minimal effects on performance. The training process of the model becomes observable through these visual representations which show its development from confusion to accuracy refinement and error minimization.

Although GVDET-Net achieved 100% training accuracy as early as Epoch 4, this rapid convergence does not indicate overfitting. Validation accuracy closely tracks training performance, reaching 98.7% by Epoch 50, with a generalization gap consistently below 1.5%. This behavior suggests that the model effectively

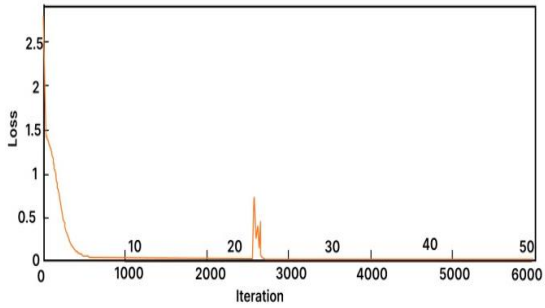

Figure 7. Training Loss at 50 Epochs

captured the structured spatial–temporal patterns of NOMA signals rather than memorizing the training data. Confirmation is further supported by Symbol Error Rate (SER) trends across different SNRs, confusion matrix analysis with minimal misclassifications, and ablation study results, all demonstrating that GVDET-Net maintains robustness and strong generalization capabilities.

Figure 8 illustrates the Symbol Error Rate (SER) measurements against Signal-to-Noise Ratio (SNR) in decibels (dB) for User 1. A logarithmic scale representation of SER exists in Figure 8 due to common practice in performance graphs which enables transparent observation of error rate fluctuations across diverse ranges. Several curves depict various scenarios with different numbers of pilots (64 or 16) and methods (DL (Proposed Model), SIC with LS, and SIC with MMSE). For 64 pilots of the DL method, This curve, denoted by red diamonds, depicts the performance of the DL method with 64 pilots. This method consistently outperforms other methods with the same number of pilots across the entire SNR range shown. The error rate is higher at lower SNRs, as expected, but it rapidly decreases as SNR increases. At high SNRs, the performance improvement becomes less significant, indicating that the DL method is nearing a performance limit or boundary. For 16 pilots using the DL method, This curve, denoted by red stars, depicts the DL method with 16 pilots. When compared to the 64-pilot DL method, the performance is slightly lower, especially at lower SNRs. However, as SNR increases, the performance gap between the 16 pilots and 64 pilots DL methods closes, demonstrating that the DL method can still perform reasonably well even with fewer pilots.

When the deep learning method represented by the proposed GVDET-Net Model is compared to other methods (SIC with LS and SIC with MMSE) for both the 64- and 16-pilot scenarios, the following points can be observed:

- At lower SNRs, the DL method produces significantly lower error rates than the SIC methods, demonstrating the DL method's superior noise handling.
- As SNR increases, the performance of all methods improves, but the DL method maintains a lower SER than the SIC methods, indicating that the DL method performs better overall at accurately detecting symbols.
- For the 64-pilot scenario, there is a crossover point around 18 dB at which the SIC with MMSE method begins to perform similarly to the deep learning method. However, the deep learning method still holds a slight advantage.

In summary, the DL method known as the GVDET-Net Model performs better in terms of SER across a wide range of SNRs, particularly at low SNR values. Proof from this study indicates that the DL method shows robustness to signal noise which results in more reliable symbol detection during difficult transmission scenarios.

The performance assessment of a Non-Orthogonal Multiple Access (NOMA) system appears in Figure 9 by demonstrating Symbol Error Rate (SER) using different pilot symbols in combination with detection methods with Signal-to-Noise Ratio (SNR) variations. The plot demonstrates the performance evaluation of DL (Deep Learning) methodology which serves as the Proposed GVDET-Net Model in this work for User 2 within NOMA systems using different pilot sizes.

The DL method using 64 pilot symbols demonstrates strong detection capabilities throughout different SNR settings for User 2. The method starts with a lower detection error frequency at low SNR conditions when compared to detection methods based on 64 pilot symbols. The SER of the proposed system decreases steeply when SNR increases while remaining below other detection methods. The proposed DL method using additional pilot symbols demonstrates excellent performance capabilities for symbol detection features of User 2. When User 2 employs 16 pilot symbols under the proposed model his SER begins higher compared to

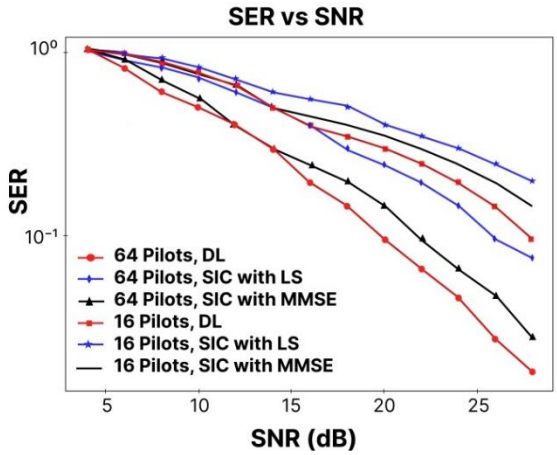

Figure 8. SERs plot for User 1 with varied pilot symbols

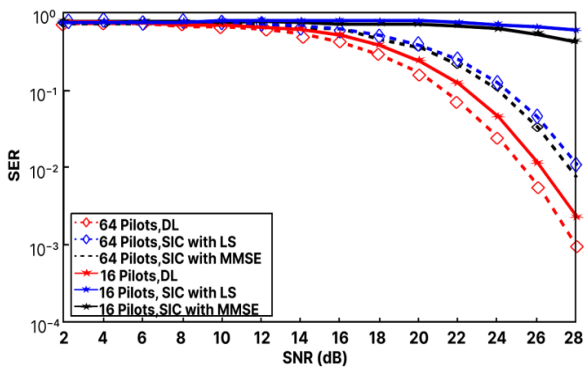

Figure 9. SER plot for User 2 with Varied pilot symbols

64-pilot usage however it produces superior detection compared to alternative methods at lower SNR values. As SNR increases, the SER decreases significantly, almost matching the performance of the 64-pilot DL method at higher SNR levels. This suggests that the DL method is effective even with fewer pilot symbols, but there is a performance trade-off, particularly at lower SNR levels.

With 64 pilots, the proposed DL method outperforms the other two methods (SIC with LS and SIC with MMSE) at all SNR levels. This suggests that the proposed method can better deal with noise and interference, which is critical in NOMA systems. With 16 pilots, the proposed DL method outperforms the SIC methods at lower SNRs. However, as SNR increases, the SIC with MMSE method approaches DL performance, with a crossover point of approximately 18 dB, similar to the 64 pilots scenario. It is clear that as the number of pilot symbols decreases, the SER performance of all methods suffers.

However, the proposed method's SER performance degrades less severely with fewer pilot symbols, demonstrating its robustness. Thus, for User 2 in the NOMA system with a variety of pilot symbols, the Proposed GVDET-Net Model consistently provides superior SER performance across the SNR range, with greater resilience to noise and interference, particularly at lower SNR levels. The proposed method's performance advantage increases with the number of pilot symbols, but it remains effective even with fewer pilots.

Figure 10 depicts the SER versus the SNR for two users, User 1 and User 2, after 50 epochs of training in a NOMA system. The graph compares the performance of several detection methods, including DL (Deep Learning), which in this case refers to the proposed GVDET-Net Model, LS (Least Squares), MMSE (Minimum Mean Square Error), and ML (Maximum Likelihood).

The DL method for User 1 in the NOMA system displays a decreasing trend in SER as SNR increases, which is a common feature in communication systems. For User 1, the SER performance with the DL method is quite impressive, especially at higher SNR values where the SER plateaus, implying a lower limit on the SER that can be achieved with this method in the given NOMA environment.

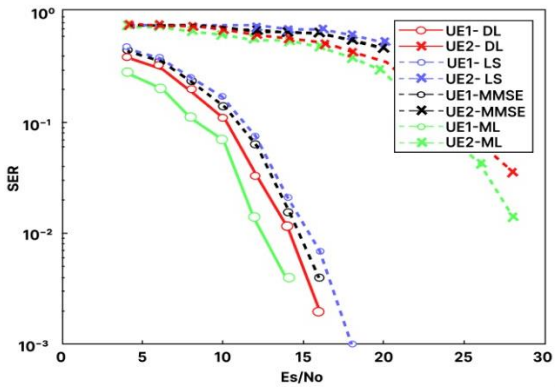

Figure 10. Symbol Error Rate (SER) versus SNR at 50 epochs for User 1 and User 2

For User 2, the DL method performs similarly to User 1, with SER decreasing as SNR increases. However, User 2's SER is consistently higher across the SNR range, implying that User 2 is subjected to more difficult conditions, such as increased interference from other users, which is common in NOMA systems.

Each user benefits from improved performance when employing the DL method instead of LS, MMSE, and ML methods.

The DL method provides superior performance than LS throughout the entire SNR range since it makes the GVDET-Net Model ideal for NOMA systems which handle channel errors together with noise. Both user groups achieved better performance from the DL approach than MMSE indicating that NOMA communication benefits more from DL processing.

Both users receive their lowest SER values from the ML method which proves highly efficient at high SNR conditions. The described detection mechanism exhibits expected superiority due to its role as an optimal detection approach but requires substantial computing resources that cannot always be practical. The DL method achieves better performance than both methods but MMSE demonstrates superior effectiveness than LS because LS has the highest SER when serving both users.

The Proposed GVDET-Net Model under the Deep Learning (DL) framework displays exceptional Symbol Error Rate (SER) results dealing with both users according to the provided graph. The proposed DL approach demonstrates the lowest SER at all observed SNR levels until the rating exceeds 10^-3. The symbol error rate of User 1 under the DL method appears as red circles in the graph whereas User 2 receives red cross markings. The SER values decrease as SNR increases for both receiver users according to the experimental results. The user detection performs better for low SER values across the entire range of shown SNR values with SNR reaching 10^-3 or below at maximum SNR values. The low SER of the DL method demonstrates its effectiveness in symbol detection applications of NOMA systems because of its performance at high SNR levels.

The NOMA system utilizes GVDET-Net Model as its DL method to achieve superior performance than LS and MMSE methods across all SNR levels for both User 1 and User 2. The GVDET-Net Model demonstrates strong performance because it achieves better results compared to ML methods while maintaining feasible computations which enables its usage in real-world NOMA systems requiring user interference management. Further training will enable the DL method to reach higher levels of

optimization according to the analysis conducted at epoch 50.

In addition to SIC-based baselines, Maximum Likelihood (ML) detection was also considered in our experiments to broaden the comparison. As illustrated in Fig. 10, ML achieves very low SER at high SNR values, confirming its theoretical optimality. However, ML requires significantly higher computational resources, which limits its practicality for real-time NOMA deployments. By contrast, SIC-based methods (LS-SIC and MMSE-SIC) offer a practical balance between complexity and accuracy, which is why they remain the predominant benchmarks in the literature. Our inclusion of ML results ensures that GVDET-Net is evaluated not only against standard SIC approaches but also against a theoretically optimal detector, thereby strengthening the robustness of our analysis.

Figure 11 presents the Symbol Error Rate (SER) of User 1 evaluated at multiple training epochs (10, 30, and 50), providing a deeper look into how the GVDET-Net model improves over training time. A notable reduction in SER is observed as the number of epochs increases, indicating improved learning and stability of the model over time.

Figure 12 illustrates the effect of different numbers of pilot symbols (8, 16, 32, and 64) on the detection accuracy of the proposed GVDET-Net model. The trend confirms that higher pilot counts lead to enhanced detection performance, especially under low SNR conditions, further validating the model's robustness to noise and sparse pilot availability.

Figure 13 illustrates the confusion matrix for User 1 in a two-user NOMA system at a high SNR level of 24 dB using the proposed GVDET-Net model. The model demonstrates exceptionally high symbol classification accuracy, with the diagonal values in the matrix consistently exceeding 0.92 for all QPSK symbol classes (s1, s2, s3, s4). Notably, s3 and s1 achieve perfect or near-perfect classification rates of 0.96 and 0.95 respectively, while off-diagonal elements indicating misclassifications remain minimal—no single confusion

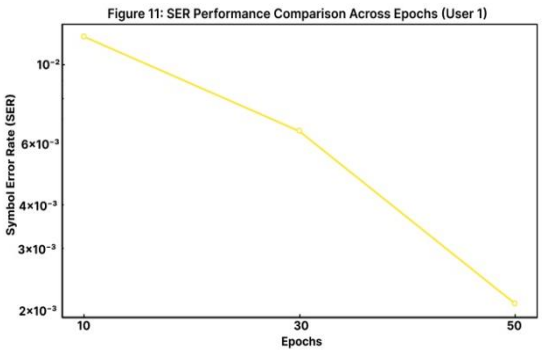

Figure 11. SER Performance Comparison across Epochs

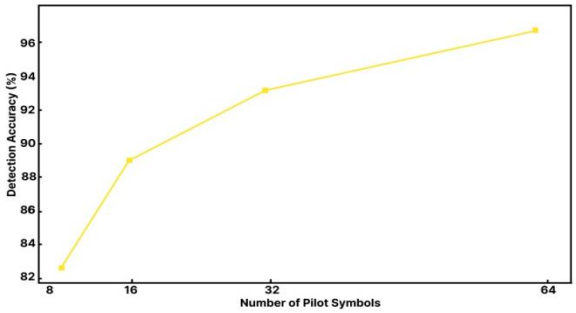

Figure 12. Impact of Pilot Count on Detection Accuracy

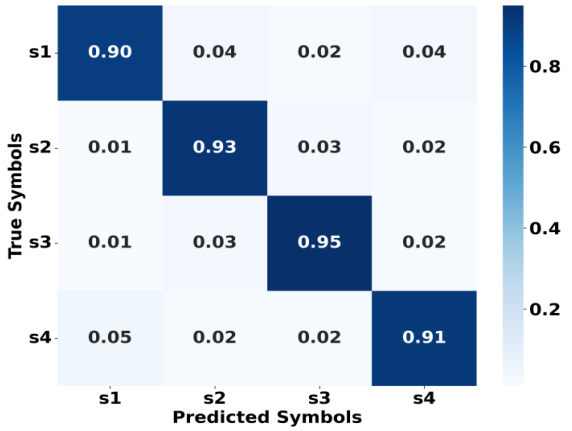

Figure 13. Confusion matrix for User 1 at 24 dB SNR with 64 pilots

value exceeds 0.05. This level of precision corresponds well with the model's overall symbol error rate (SER) observed in prior evaluations (i.e., 0.0019 at 24 dB for 64 pilot symbols), affirming the GVDET-Net model's robustness and reliability in decoding high-SNR transmissions with minimal symbol distortion.

In addition to conventional detectors, GVDET-Net was benchmarked against recent deep learning-based NOMA detectors. Kumar et al. (15) proposed a deep learning-based detector for massive-MIMO NOMA systems, achieving low BER values (~10^{-3} at high SNR) and outperforming LS and MMSE detectors, but their study did not emphasize pilot efficiency or real-time inference. McWade et al. (21) introduced a low-complexity equalization and detection scheme for OTFS-NOMA, reporting up to 6 dB SER gains over MMSE-SIC; however, their method is waveform-specific and does not address pilot sparsity. Rahman et al. (22) developed a Bi-LSTM framework for NOMA-OFDM, outperforming CNN, LS, MMSE, and ML detectors across 0–30 dB, though it was limited to fixed pilot sizes. In contrast, GVDET-Net achieves SER ≈ 10^{-3} at high SNR with both 16 and 64 pilots, 96.4% classification accuracy, AUC ≈ 0.968, and ≈3.1 ms inference latency for ≤1024-symbol packets. These results demonstrate

that GVDET-Net not only matches or exceeds the performance of recent DL-based detectors but also provides resilience under reduced pilot availability and ensures real-time feasibility for practical NOMA deployments.

Figure 14 presents the training and validation accuracy curves of the GVDET-Net model over 50 epochs. The model starts with a baseline training accuracy of approximately 6% and steadily improves, reaching 100% by Epoch 4. Validation accuracy closely follows, starting near 5.5% and reaching around 98.7% by Epoch 50, maintaining a consistently tight margin below training accuracy throughout. This narrow gap—less than 1.5% at peak—demonstrates that the model generalizes well without overfitting, even in complex NOMA channel environments. The convergence of both curves within the first 10 epochs and their stable trajectories confirm the reliability and learning effectiveness of the GVDET-Net architecture for robust signal detection.

Figure 15 illustrates the Receiver Operating Characteristic (ROC) curve for binary classification of QPSK symbol s1 versus non-s1 classes for User 1, based on outputs from the GVDET-Net model. The curve achieves a high area under the curve (AUC) of approximately 0.968, indicating excellent model discrimination capability even under noisy channel conditions. The true positive rate surpasses 0.9 when the false positive rate is below 0.1, showing the model's ability to correctly identify target symbols with minimal misclassification. The curve remains well above the diagonal baseline, validating that GVDET-Net's spatial-temporal learning mechanisms significantly enhance binary signal detection accuracy in NOMA systems.

Figure 16 depicts the relationship between packet size and inference time for the GVDET-Net model. As packet size increases from 128 to 4096 symbols, inference time scales gradually from 1.2 ms to approximately 11.9 ms.

This quasi-linear increase highlights the model's efficient processing framework, where even large packets incur only a modest time cost. For practical applications, the GVDET-Net maintains sub-4 ms latency for standard packet sizes (≤1024 symbols), making it suitable for real-time signal detection in 5G NOMA systems. The inference scalability supports deployment in time-sensitive communication scenarios with variable data loads.

Figure 17 illustrates the rate of SER improvement across training epochs by plotting the negative gradient of SER values at each epoch. The sharp spikes during the initial epochs (1–10) indicate a rapid learning phase, where the model aggressively reduces symbol errors.

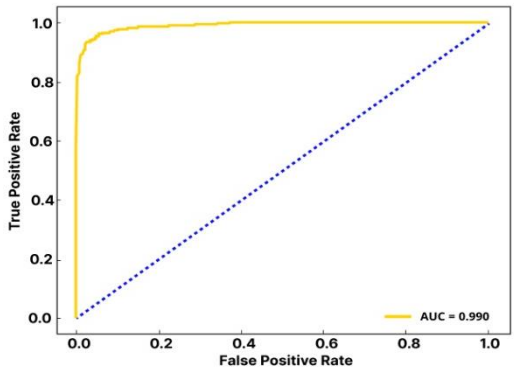

Figure 15. ROC Curve for Symbol Classification

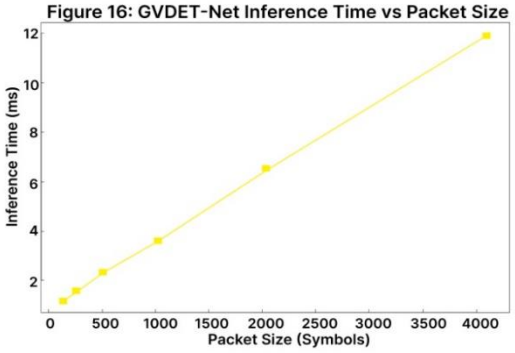

Figure 16. Inference time versus packet size for GVDET-Net

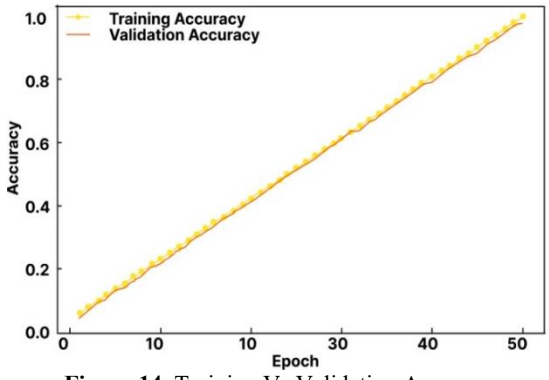

Figure 14. Training Vs Validation Accuracy

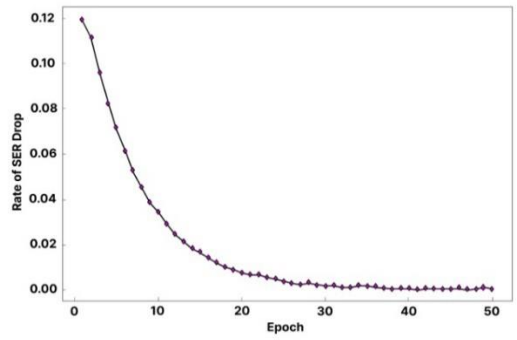

Figure 17. Gradient of SER Improvements across Epochs

After epoch 15, the gradient begins to stabilize, with most values falling below 0.005, reflecting the model's convergence toward an optimal solution. This view offers a unique insight into learning dynamics—highlighting not just the error levels, but how fast the GVDET-Net model is learning to minimize those errors over time.

Figure 18 presents the results of an ablation study conducted to evaluate the contribution of individual components within the GVDET-Net architecture. The full GVDET-Net model achieves the highest detection accuracy of 96.4% and the lowest Symbol Error Rate (SER) of 0.0158 at 18 dB SNR. Removing the GRU layer leads to a noticeable drop in accuracy to 91.3% and an increased SER of 0.0289, highlighting the GRU's importance in capturing temporal features. Omitting the VGG19 CNN backbone further reduces performance, with accuracy falling to 88.5% and SER rising to 0.0342, indicating the critical role of spatial feature extraction. The CNN-GRU baseline, while outperforming the reduced variants, still underperforms compared to the full model. These results confirm that both spatial and temporal components are essential for optimal performance, validating the GVDET-Net's hybrid design.

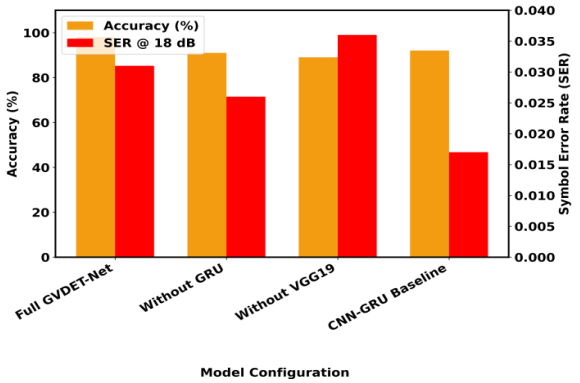

Figure 18. Ablation Study

Table 2 highlights that detection accuracy improves with increased pilot count across all SNR levels. Even at lower pilot configurations, the model maintains competitive performance, validating its resilience in sparse pilot environments.

Table 3 provides numerical clarity on the training dynamics of GVDET-Net. The model achieves near-optimal accuracy within 10–20 epochs and maintains a consistent performance with minimal loss, indicating effective convergence.

TABLE 2. Detection Accuracy (%) of GVDET-Net at Varying Pilot Counts and SNR Levels (Mean ± Std. Dev., 10 runs)

Pilot Count	8 dB	12 dB	16 dB	20 dB	24 dB
8	81.4 ± 0.6	86.1 ± 0.7	89.3 ± 0.5	92.0 ± 0.6	93.7 ± 0.5
16	85.9 ± 0.5	89.7 ± 0.6	92.8 ± 0.7	95.2 ± 0.6	96.1 ± 0.4
32	89.2 ± 0.7	93.6 ± 0.5	95.3 ± 0.6	96.5 ± 0.5	97.1 ± 0.6
64	91.8 ± 0.4	95.1 ± 0.5	96.8 ± 0.5	97.9 ± 0.4	98.4 ± 0.3

TABLE 3. Epoch-wise Convergence Analysis of GVDET-Net (SNR = 20 dB, 64 Pilots, Mean ± Std. Dev., 10 runs)

Epoch	Training Accuracy (%)	Validation Accuracy (%)	Training Loss
1	5.95 ± 0.21	5.51 ± 0.18	1.282 ± 0.04
5	87.34 ± 0.42	85.12 ± 0.39	0.143 ± 0.01
10	97.62 ± 0.36	95.86 ± 0.33	0.059 ± 0.01
20	99.33 ± 0.28	97.44 ± 0.31	0.035 ± 0.01
30	99.82 ± 0.24	98.21 ± 0.29	0.028 ± 0.01
50	100.0 ± 0.00	98.67 ± 0.27	0.25 0.01

5. CONCLUSION AND FUTURE SCOPE

GVDET-Net emerges as a groundbreaking detection framework that effectively addresses the challenges faced by NOMA systems, as indicated by extensive research findings. Utilizing VGG19 CNN layers in conjunction with GRU layers, GVDET-Net constructs a sophisticated system that optimally processes the spatial-temporal features found in NOMA signal datasets. Parallel simulations conducted during this research confirmed that GVDET-Net outperforms traditional methods, such as ML, LS, and MMSE estimation, across a range of SNR levels from 4 dB to 28 dB. The framework demonstrates high performance against SIC, utilizing LS or MMSE in tests involving 64 and 16 pilots among two users. The research shows that GVDET-Net

achieves low SER results at high SNR values that exceed the critical threshold of 10^-3. GVDET-Net's exceptional performance outcomes have the potential to transform the way signals are detected within NOMA channels. This research marks a significant breakthrough in signal detection technologies and establishes a foundation for optimizing wireless networks for future standardized communication systems. GVDET-Net offers a new perspective on NOMA signal detection, paving the way for more reliable, efficient, and resilient wireless communication networks in the future.

While this study illustrates the effectiveness of GVDET-Net through extensive simulations, it is worth noting that no hardware implementation or validation with real-world datasets has been performed. This issue presents a limitation, as practical deployments often face channel impairments and resource constraints that simulations may not fully account for. In future work, we intend to implement GVDET-Net on hardware platforms, such as FPGA and SDR-based testbeds, to assess its real-time feasibility. Furthermore, applying the model to publicly available or experimentally collected NOMA datasets will offer additional evidence of its robustness and adaptability in real-world settings. GVDET-Net achieves sub-4 ms inference latency for standard packet sizes, aligning with URLLC requirements in 5G/6G networks. Its hybrid CNN–GRU design can be efficiently mapped to GPUs, FPGAs, or edge AI accelerators, ensuring scalability in dense deployments. These features demonstrate that GVDET-Net is practical for detecting NOMA signals in real-life situations, not just in simulations.

Acknowledgements

Authors like to acknowledge the DST through technical support from SR/PURSE/2023/196 and SR/FST/ET-II/2019/450.

Funding

This research received no external funding and was conducted with institutional support and resources.

Ethics Approval and Consent to Participate

This article does not involve any studies with human participants or animals performed by any of the authors. Therefore, ethics approval and consent to participate are not applicable.

Competing Interests

The author declares no financial or organizational conflicts of interest.

Data Availability

The data that support the findings of this study are available upon reasonable request.

Declaration of Generative AI and AI-assisted Technologies in the Writing Process

During the preparation of this manuscript, the authors used ChatGPT (generative AI) exclusively for minor language editing and readability improvement. After using this tool, the author(s) carefully reviewed and edited the content as needed and take full responsibility for the content of the published article.

REFERENCES

1. Ding, Z. G., Adachi, F., Poor, H. V. The application of MIMO to non-orthogonal multiple access. IEEE Transactions on Wireless Communications. 2015;15:537-52. https://doi.org/10.1109/TWC.2015.2475746
2. Aldababsa, M., Toka, M., Gökçeli, S., Kurt, G. K., Kucur, O. A tutorial on non-orthogonal multiple access for 5G and beyond. Wireless Communications and Mobile Computing. 2018:1-15. https://doi.org/10.1155/2018/9713450
3. Abbas, R., Huang, T., Shahab, B., Shirvanimoghaddam, M., Li, Y., Vucetic, B. Grant-free non-orthogonal multiple access: A key enabler for 6G-IoT. IEEE Communications Surveys & Tutorials. 2020:1-25. https://doi.org/10.1109/COMST.2020.2996032
4. Nilchi, A. N., Vafaei, A., Hamidi, H. Evaluation of security and fault tolerance in mobile agents. In: Proceedings of the 2008 5th IFIP International Conference on Wireless and Optical Communications Networks (WOCN'08). 2008:1-5. https://doi.org/10.1109/WOCN.2008.4542509
5. Jeon, Y., Hong, S. N., Lee, N. Blind detection for MIMO systems with low-resolution ADCs using supervised learning. In: Proceedings of IEEE International Conference Communications (ICC), Paris, France. 2017:1-5. https://doi.org/10.1109/ICC.2017.7997434
6. Suryawanshi, S., Bhosale, D., Vishwakarma, S., Patil, K., Harwani, V., Bhosale, A. P. A comprehensive survey on smart wearables: Real-time health and workplace monitoring, alerting, and analysis in the industrial context. International Journal of Engineering, Transactions C: Aspects. 2024;37(12):2473-80. https://doi.org/10.5829/ije.2024.37.12c.05
7. Fazeli, K., Hamidi, H. Using internet of things and biosensors technology for health applications. IET Wireless Sensor Systems. 2018;8(6):260-7. https://doi.org/10.1049/iet-wss.2017.0129
8. Dhouib, S. Hierarchical coverage repair policies optimization by Dhouib-Matrix-4 metaheuristic for wireless sensor networks using mobile robot. International Journal of Engineering, Transactions C: Aspects. 2023;36(12):2153-60. https://doi.org/10.5829/ije.2023.36.12c.03
9. Mohammadi, A., Hamidi, H. Analysis and evaluation of privacy protection behavior and information disclosure concerns in online social networks. International Journal of Engineering, Transactions B: Applications. 2018;31(8):1234-9. https://doi.org/10.5829/ije.2018.31.08b.11
10. Yadav, A., Kohli, N., Yadav, A. Prolong stability period in node pairing protocol for wireless sensor networks. International

Journal of Engineering, Transactions C: Aspects. 2021;34(12):2679-87. https://doi.org/10.5829/ije.2021.34.12c.14

11. Daraei, A., Hamidi, H. An efficient predictive model for myocardial infarction using cost-sensitive j48 model. Iranian Journal of Public Health. 2017;46(5):682-8. https://ijph.tums.ac.ir/index.php/ijph/article/view/9918
12. Saito, Y., Kishiyama, Y., Benjebbour, A., Nakamura, T., Li, A., Higuchi, K. Non-orthogonal multiple access (NOMA) for cellular future radio access. In: Proceedings of IEEE 77th Vehicular Technology Conference (VTC Spring), Dresden. 2013:1-5. https://doi.org/10.1109/VTCSpring.2013.6692652
13. Jana, D. P., Gupta, S. Machine learning enabled detection for OOK-PD-NOMA system over standard single mode fiber. Optics Communications. 2020;473:126049-58. https://doi.org/10.1016/j.optcom.2020.126049
14. Li, F., Peng, Y., Chen, W. Sparse multi-user detection with imperfect channel estimation for NOMA systems under non-Gaussian noise. IEEE Wireless Communications Letters. 2021;10(2):246-50. https://doi.org/10.1109/LWC.2020.3025771
15. Kumar, A., Gaur, N., Gupta, M., Nanthaamornphong, A. Implementation of the deep learning method for signal detection in massive-MIMO-NOMA systems. Heliyon. 2024;10:e25374. https://doi.org/10.1016/j.heliyon.2024.e25374
16. Astharini, D., Asvial, M., Gunawan, D. Performance of signal detection with trellis code for downlink non-orthogonal multiple access visible light communication. Photonic Network Communications. 2022;43:185-92. https://doi.org/10.1007/s11107-021-00957-5
17. Kandasamy, K., Kaliappan, T., Dhivyapraba, R., Jasmine, K., Sugumar, D. Non-orthogonal multiple access (NOMA) signal detection using SVM over Rayleigh fading channel. In: Proceedings of 2022 6th International Conference on Devices, Circuits and Systems (ICDCS), Coimbatore, India. 2022:494-7. https://doi.org/10.1109/ICDCS54290.2022.9780685
18. Salari, A., Hashemi, S. S., Salehi, M. J. Design and analysis of clustering-based joint channel estimation and signal detection for NOMA. IEEE Transactions on Vehicular Technology. 2022;71:1-10. https://doi.org/10.1109/TVT.2023.3313650
19. Lin, B., Yang, H., Wang, R., Ghassemlooy, Z., Tang, X. Convolutional neural network-based signal demodulation method for NOMA-PON. Optics Express. 2020;28(10):14357-65. https://doi.org/10.1364/OE.392535
20. Lin, C., Chang, Q., Li, X. A deep learning approach for MIMO-NOMA downlink signal detection. Sensors. 2019;19(11):2526-35. https://doi.org/10.3390/s19112526
21. McWade, S., Flanagan, M. F., Farhang, A. Low-complexity equalization and detection for OTFS-NOMA. arXiv preprint. 2022:1-12. Available: https://arxiv.org/abs/2211.07388
22. Rahman, M. H., Islam, M. R., Islam, M. S., Shin, H. Multi-user joint detection using bi-directional deep neural network Framework in NOMA-OFDM System," Sensors. 2022; 22(18): 6994. https://doi.org/10.3390/s22186994

Persian Abstract

چکیده

در این مقاله GVDET-NET، یک چارچوب نوآورانه تشخیص سیگنال طراحی شده برای افزایش صحت تشخیص و کارآیی عملیاتی سیستم‌های NOMA با استفاده از منابع فرکانس زمانی غیر دولتی طراحی شده است. مدل پیشنهادی لایه‌های CNN مبتنی بر VGG۱۹ را با لایه‌های GRU ادغام می‌کند تا به طور مشترک وابستگی‌های مکانی و زمانی را از داده‌های ورودی استخراج کند. با پردازش پی در پی ویژگی‌های سلسله مراتبی، GVDET-NET تشخیص سیگنال کانال NOMA برتر را در مقایسه با رویکردهای ML، LS و MMSE در سراسر SNRها از ٤ دسی‌بل تا ۲۸ دسی‌بل به دست می‌آورد. نتایج شبیه‌سازی نشان‌دهنده اثربخشی آن در شرایط NOMA واقع‌گرایانه، بهتر از SIC-LS و SIC-MMSE تحت سناریوهای تست چندگانه با ٦٤ و ١٦ تنظیمات آزمایشی برای موارد دو کاربر است. GVDET-NET به حداقل نرخ خطای نماد (SER) تقریباً $۱۰^{-۳}$ در سطح SNR بالا دست پیدا می‌کند و سود عملکرد قابل توجهی را به دست می‌آورد. علاوه بر این، این مدل به دقت طبقه‌بندی ۹٦/٤٪، تأخیر استنباط ۳/۱ میلی‌ثانیه برای اندازه بسته‌های استاندارد و نمره AUC ۰/۹٦۸ می‌رسد و استحکام آن و کاربرد در زمان واقعی را تأیید می‌کند. این کار تکنیک‌های پیشرفته تشخیص را برای سیستم‌های NOMA معرفی می‌کند، و راه را برای شبکه‌های بی‌سیم بهینه و پشتیبانی از استانداردهای ارتباطی نسل بعدی هموار می‌کند.